Journal of Electron Microscopy Advance Access published April 27, 2009
Journal of Electron Microscopy: 1–9 (2009)
doi: 10.1093/jmicro/dfp021

Special number: Instrumentation/Performance

First application of C_c-corrected imaging for high-resolution and energy-filtered TEM

Bernd Kabius[1,*], Peter Hartel[2], Maximilian Haider[2], Heiko Müller[2], Stephan Uhlemann[2], Ulrich Loebau[2], Joachim Zach[2] and Harald Rose[3]

[1]Argonne National Laboratory, 9700 South Cass Avenue, Argonne 60439, IL, USA, [2]CEOS GmbH, Engeler Strasse 28, D-69126 Heidelberg and [3]Technical University Darmstadt, D-64289 Darmstadt, Germany
*To whom correspondence should be addressed. E-mail: kabius@anl.gov

Abstract Contrast-transfer calculations indicate that C_c correction should be highly beneficial for high-resolution and energy-filtered transmission electron microscopy. A prototype of an electron optical system capable of correcting spherical and chromatic aberration has been used to verify these calculations. A strong improvement in resolution at an acceleration voltage of 80 kV has been measured. Our first C_c-corrected energy-filtered experiments examining a $(LaAlO_3)_{0.3}(Sr_2AlTaO_6)_{0.7}/LaCoO_3$ interface demonstrated a significant gain for the spatial resolution in elemental maps of La.

Keywords aberration correction, chromatic aberration, oxides, EFTEM, HRTEM

Received 17 December 2008, accepted 30 March 2009

Introduction

One of the most challenging tasks for transmission electron microscopy (TEM) is the investigation of the atomic structure and chemistry of nano-scale structures. These properties are important to expand our understanding of the novel physical phenomena that are exhibited by nano-scale heterostructures. These materials provide an avenue to combine dissimilar materials with different and often antagonistic order parameters that can lead to qualitatively new behavior. For example, quantum tunneling across a thin oxide layer can be controlled by the magnetic state of the material on either side or by the spin polarization of the interfaces, or new strongly correlated states can be created at the interface between two different complex oxides. However, exploring and developing the properties of confined quantum mechanical systems places ever-increasing demands on materials and requires atomic-level knowledge of the interfaces and surfaces in order to predict and control their physical properties. Likewise, such knowledge is critical to enhance our fundamental understanding of the origins of the novel physics and chemistry that are observed at nano-scale interfaces. Precise knowledge about the position of each atom as well as the local chemistry is crucial to answer the questions mentioned above. This analytical requirement was raised by Richard Feynman in his famous 1959 lecture, 'There's plenty of room at the bottom' [1].

The TEAM project (Transmission Electron Aberration-corrected Microscope) was initiated to address Feynman's challenge [2–4]. An important topic for the TEAM project was also improving the quality of electron optical imaging for *in situ* experiments. To achieve this goal, improvement of the electron optical system as well as improved high-stability sample stages and high-brightness electron emitters was envisioned. The resolution goal of the TEAM project was set to 0.5 Å in the TEM and STEM mode to be able to resolve crystal lattices even along high-indexed zone axes and to achieve single-atom sensitivity. This resolution should be available using an objective lens with a relatively large pole-piece gap of ~5 mm to allow tomography and various *in situ* experiments. Correction of spherical aberration C_s has been demonstrated for high-resolution TEM (HRTEM) [5] and promised novel abilities for TEM experiments, and is therefore part of the instrument concept. Correction of chromatic aberration (C_c) was assumed to be beneficial for *in situ* experiments because it would allow for objective lenses with a large pole-piece gap without compromising resolution. Development of an electron optical system capable of C_c correction is one of the key components of the TEAM project. Further benefits of C_c correction were expected for energy-filtered TEM (EFTEM), for imaging thick samples and for HRTEM at acceleration voltages below 120 kV [6]. The first prototype of an electron optical system

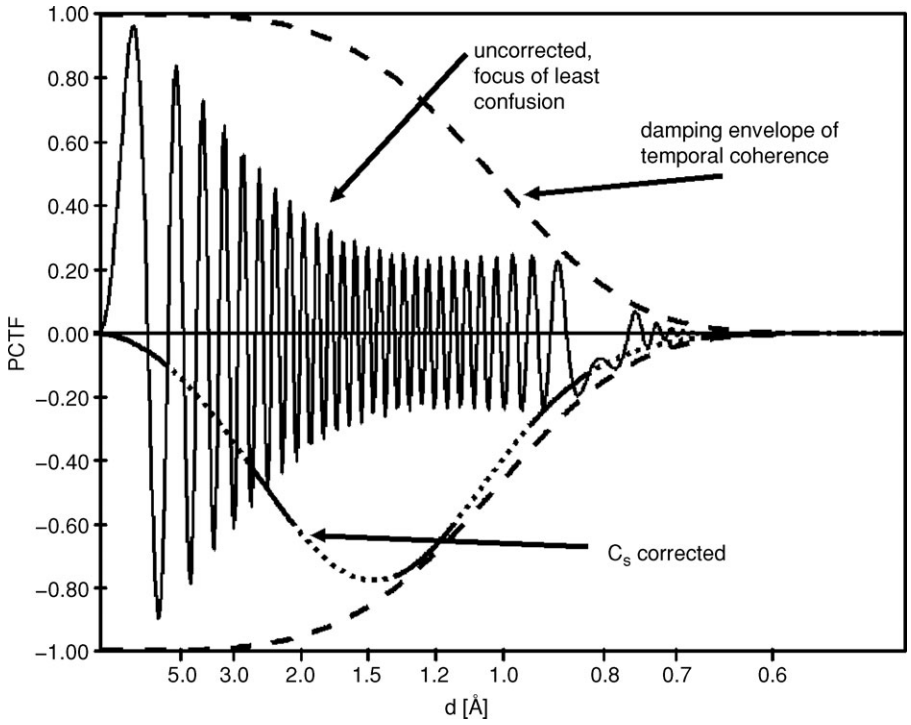

Fig. 1. Contrast transfer for uncorrected and C_s-corrected TEMs for an electron energy of 300 kV.

with correction of C_s and C_c has been developed by CEOS GmbH (Heidelberg, Germany) [7] and was integrated into an FEI Titan microscope. First experiments with this novel aberration corrector have been performed and demonstrated successful correction of C_c and several of its benefits for material science applications.

Method

To date different instruments have been used for HRTEM and *in situ* studies. The major difference in the electron optics system of these microscopes is the objective lens. To achieve optimum spatial resolution, the gap between the pole pieces of the objective lens has to be very small (2–3 mm) to minimize spherical and chromatic aberration and allow sub-Angstrom (sub-Å) resolution by phase reconstruction [8], holography [9] or C_s correction. Similar results have been achieved in the STEM mode [10]. The phase contrast transfer functions (PCTFs) for an uncorrected and a C_s corrected microscope and the damping envelope of temporal coherence of such an instrument are plotted in Fig. 1 and demonstrate an information limit of 0.7–0.8 Å. An acceleration voltage of 300 kV has been assumed for these calculations. The lens parameters are $C_s = 0.6$ mm, $C_c = 1.6$ mm, semi-convergence angle = 0.1 mrad, $C_5 = 4$ mm, energy spread of the electron beam $\Delta E = 0.7$ eV. The value for chromatic aberration includes the relativistic correction for 300-keV electrons [11]. The focus of least confusion for $g_{\max} = 0.75$ Å was assumed for the uncorrected state. The damping envelope of temporal coherence was calculated with the same set of parameters. A C_s corrector adds ~0.2 mm to the value of chromatic aberration, which is taken into account for the PCTF of the corrected instrument. The value for defocus and C_s was chosen according to Scherzer [12] to balance defocus, C_s and C_5 for maximum phase contrast. The C_s-corrected instrument can be operated with homogeneous contrast transfer up to the information limit while interpretation of images recorded with the uncorrected microscope requires extensive calculations, such as phase reconstruction [13].

These small-gap objective lenses enabled sub-Å resolution, but they severely restricted space around the sample and limited the capabilities of the instrument for methods other than high-resolution imaging. Tilt angles are limited to about ±20° using a sample with a diameter of 3 mm. Therefore, tomographic tilt series are restricted severely as well as many other experiments necessary for *in situ* studies. An objective aperture cannot be placed in the back focal plane, which hampers diffraction contrast imaging. Space for further experimental equipment, such as liquid cells, tips for electrical measurement or magnetic coils, is very limited.

An objective lens with a gap of ~5 mm offers much better capabilities for a wide range of experiments and was therefore chosen for the first instrument of the TEAM project. The tilt range increases by a factor of 2 for standard sample holders. Custom-built holders allow a 360° rotation, thus avoiding the 'missing wedge' problem for tomographic experiments. This type of objective lens has already demonstrated that it can be used for various *in situ* applications such as the study of thin-film growth [14] and electrochemical reactions in a liquid cell [15].

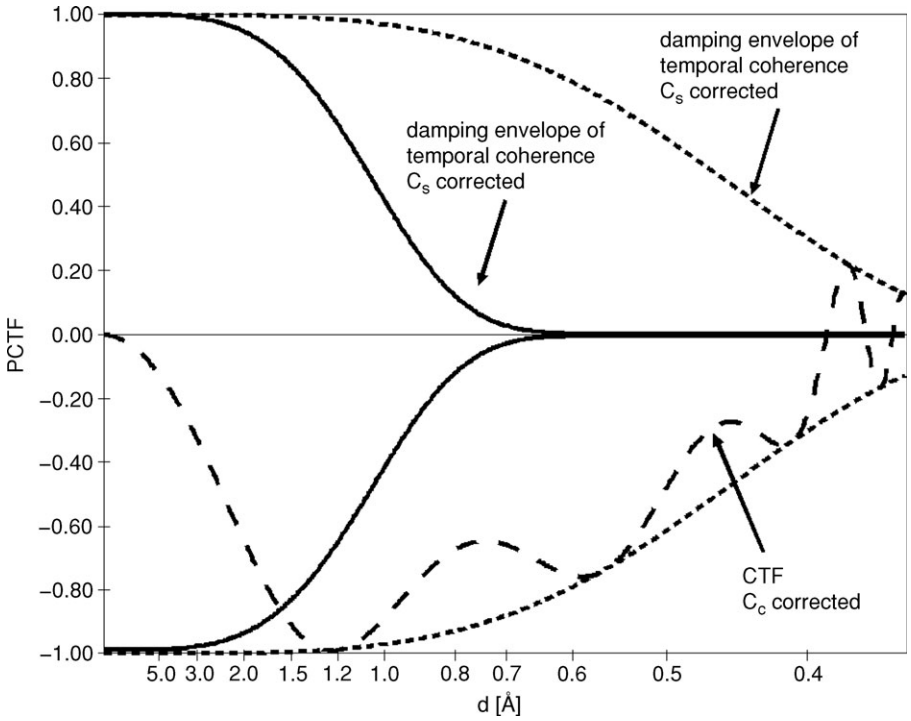

Fig. 2. Information limit of a C_s-corrected (black) and a C_c-corrected TEM (blue) at 300 kV.

Spatial resolution for this type of objective lens cannot be improved by C_s correction alone as the information limit is set by the damping envelope of temporal coherence, which is a function of acceleration voltage and defocus spread d_s. For a given acceleration voltage, the damping envelope is determined by the defocus spread [see Eq. (1)]:

$$d_s = \sqrt{\left(d_s^Q \frac{2\Delta I_Q}{I_Q}\right)^2 + \left(d_E^Q \frac{\Delta E_Q}{E_Q}\right)^2 + \left(C_c \sqrt{\left(\frac{\Delta E}{E}\right)^2 + \left(\frac{\Delta H}{H}\right)^2 + \left(\frac{2\Delta I}{I}\right)^2}\right)^2}, \quad (1)$$

where

ΔI_Q represents the instabilities of the electrical current of the magnetic quadrupoles of a C_c corrector,

d_s^Q is the proportionality constant between ΔI_Q and defocus,

ΔE_Q represents instabilities of the voltage of the electric quadrupoles of a C_c corrector,

d_E^Q is the proportionality constant between ΔE_Q and defocus,

ΔE is the energy spread of the electron emitter,

ΔH is the instability of the acceleration voltage and

ΔI is the instability of the objective lens current.

Equation (1) is an extension of the expression which can be found in the literature [16]. The first two terms take the instabilities of power and voltage supplies for the multipoles of the C_c corrector into account. The stability of the objective lens current I and the acceleration voltage H is already close to 10^{-7} and further improvement does not extend the information limit significantly. Chromatic aberration and energy spread of the emitter are the two parameters in Eq. (1) which have a strong effect on the information limit. These parameters lead to the two concepts which are employed by the TEAM project for enhancing resolution: C_s correction with electron beam monochromatization and C_c and C_s correction (referred to as C_c correction in the following). The first concept is based on available technology, and was included as a fallback solution because of the high risk related to the development of a C_c corrector. The major risks were the high complexity of the electron optical system and the high demands on power and voltage supply stability of ~0.01 ppm [17]. The calculations of temporal coherence displayed in Fig. 2 demonstrate the advantage of C_c correction over C_s correction with respect to spatial resolution. Improving C_c from 2.0 mm to 10 μm improves the information limit from 0.8 Å to better than 0.5 Å. A PCTF is included in Fig. 2 which has been calculated under the assumption that the voltage and power stabilities mentioned above are met. The damping envelope of temporal coherence takes corrector instabilities [Eq. (1)] and a residual C_c of 10 μm into account.

Energy monochromatization and C_c correction result in a similar contrast transfer at 300 kV if an energy width of 0.1 eV can be achieved. Whether this potential of C_c correction can be verified depends on several parameters which are either difficult to quantify or depend on the environment of the instrument, such as floor vibrations or further instabilities in the electron optical or mechanical system. The fallback solution, C_s corrector and a monochromator, has already demonstrated that an information limit of 0.5 Å can be achieved [18]. Apart from HRTEM at 300 kV,

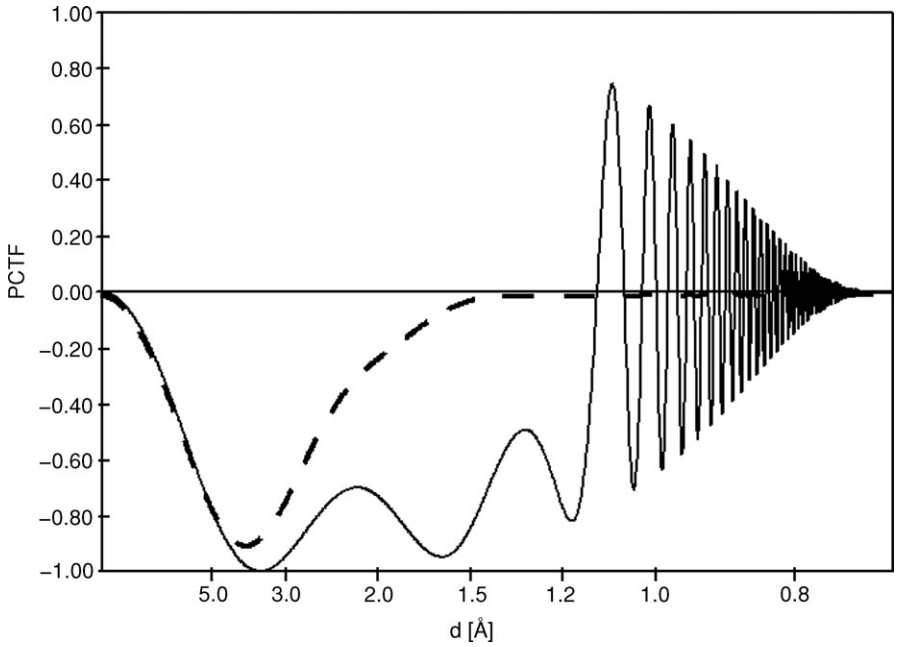

Fig. 3. Contrast transfer at 30 kV for a monochromatic (dashed line) and a C_c-corrected (solid line) TEM.

C_c correction has several advantages as compared to monochromatization. C_c correction does not alter the properties of the electron beam source. Therefore, the brightness of the electron source is undiminished and the full beam current of a Schottky emitter (~100 nA) can be used, while a monochromatic system diminishes the beam current significantly. Monochromatization improves the energy width ΔE by about an order of magnitude while C_c can be improved by three orders of magnitude to a few micrometers. The advantage in contrast transfer for HRTEM is small at 300 kV, but increases at lower acceleration voltages as can be seen in Fig. 3. These PCTFs have been calculated for 30 kV and show sub-Å resolution with a much higher contrast transfer for the C_c-corrected system. For experiments where the energy width of the electron beam is inherently large, such as EFTEM or observation of thick samples, monochromatization is ineffective but C_c correction has a strong impact on spatial resolution.

Results and discussion

An electron optical system capable of correcting spherical and chromatic aberration has been developed by CEOS GmbH for the TEAM project. The design requirements for this corrector have already been described in detail [7]. The first prototype is now integrated into an FEI Titan microscope with a Supertwin lens with a C_s of 1.2 mm and a C_c of 2.0 mm at 300 kV. The instrument is equipped with a post-column energy filter (Gatan GIF Tridiem 863). Young's fringe tests using a thin layer of amorphous tungsten on amorphous carbon films were used to measure information limits without aberration correction of 0.9 Å at 300 kV and 1.8 Å at 80 kV acceleration voltages. C_c was measured by recording two images of the same sample area with the same objective lens current at two different acceleration voltages. Then the focus difference induced by the voltage change between the two images was calculated and C_c was determined according to Eq. (2):

$$C_c = \frac{df * H}{dH}. \tag{2}$$

A value of 2 ± 1.5 μm for C_c was measured at 80 kV, and is an improvement of three orders of magnitude compared to the C_c of 1.4 mm for the uncorrected objective lens at 80 kV. The measurement error is determined by the accuracy of defocus measurement and high voltage instability. Spherical and axial aberration parameters were measured from Zemlin tableaus [19] and were compensated up to third order and optimized up to fifth order.

An information limit measurement with the Young fringe method (Fig. 4) shows contrast transfer up to 1.0 Å and is a significant improvement compared to the information limit of 1.8 Å which can be achieved with a C_s-corrected or an uncorrected microscope. This result is nearly identical to the information limit of the microscope measured at 300 kV (0.9 Å). Contrast-transfer calculations show that further progress in resolution can be expected from the C_c corrector if the stability of the microscope and the corrector is improved (Fig. 2).

Energy-filtered imaging should benefit strongly from C_c correction as mentioned above. The effective beam energy width for unfiltered HRTEM, which is used for Eq. (1), is the FWHM width of the zero-loss beam. This is correct for thin samples where the majority of the electrons are elastically scattered. An energy selection aperture with a certain width is used for recording energy-filtered images and positioned

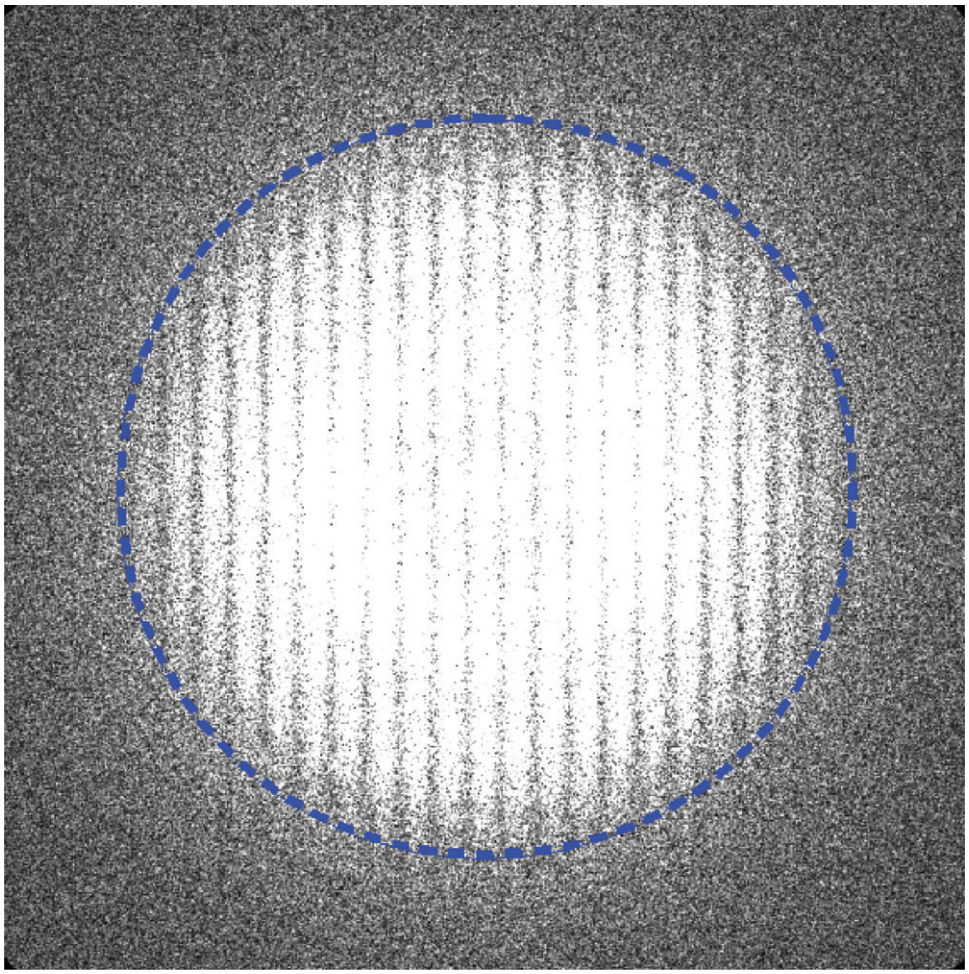

Fig. 4. Young fringe test at 80 kV with C_c correction. The dashed circle marks 1.0 Å.

at a certain energy loss. In this case, ΔE can be approximated by the width of the energy selection aperture under the assumption that the electron energy distribution within the aperture is homogeneous. The width of the energy selection aperture is usually set to values between 5 and 50 eV in order to achieve a reasonable signal-to-noise ratio. Furthermore, a high beam convergence is necessary to collect a sufficient number of electrons. Both parameters, energy width as well as beam convergence, reduce spatial resolution significantly. Figure 5 shows calculations of the damping envelopes of the PCTF, temporal as well as spherical, for conditions which are suitable for energy-filtered imaging with the La–M transition at 832 eV: semi-convergence angle s_c = 3 mrad, width of the energy selection aperture dE = 50 eV, acceleration voltage HT = 200 kV.

Standard values for C_s (1.2 mm) and C_c (1.6 mm) for the Supertwin lens have been assumed for the uncorrected system. C_1, C_s and C_5 have been balanced according to Scherzer [12] to minimize the influence of the damping envelope of spherical coherence for the C_s-corrected instrument. The values for the spherical aberration constants C_s and C_5 for the C_c-corrected case have been measured from Zemlin tableaus recorded with the C_c-corrector prototype at 200 kV to be 9 μm and −3 mm, respectively. Measurement of C_c resulted in 5 μm. We conclude from these calculations that the influence of C_c is much stronger than that of beam convergence and C_s making a C_c corrector more efficient than a C_s corrector for improving the spatial resolution of energy-filtered images. Contrast transfer for a C_c-corrected system is larger than 10% up to 1.2 Å. The resolution which can be achieved for elemental mapping is therefore no longer limited by electron optics, but by the signal-to-noise ratio and sample drift.

These improved elemental mapping capabilities can be demonstrated with an elemental map of La calculated from energy-filtered images recorded at the La–M transition. The delocalization of this energy-loss process can be calculated to 1.8 Å [20,21] and is small enough to allow atomic-scale resolution. Figure 6 shows a HRTEM image of a cross-sectional sample of $LaAlO_3$ on LSAT $(LaAlO_3)_{0.3}(Sr_2AlTaO_6)_{0.7}$. An ordered structure caused by O-deficiency can be seen in the $LaCoO_3$ film [22] (arrows in the inset of Fig. 6).

The same area shown in Fig. 6 has been used for C_c-corrected elemental mapping (see Fig. 7, right-hand side).

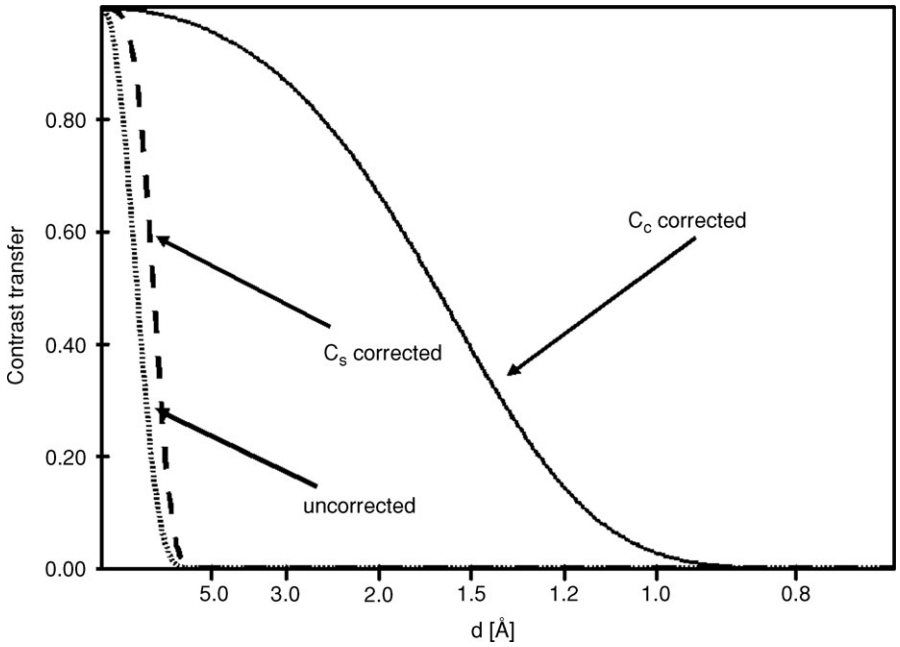

Fig. 5. Damping envelopes of spatial and temporal coherence for parameters suitable for mapping of La using the La–M transition.

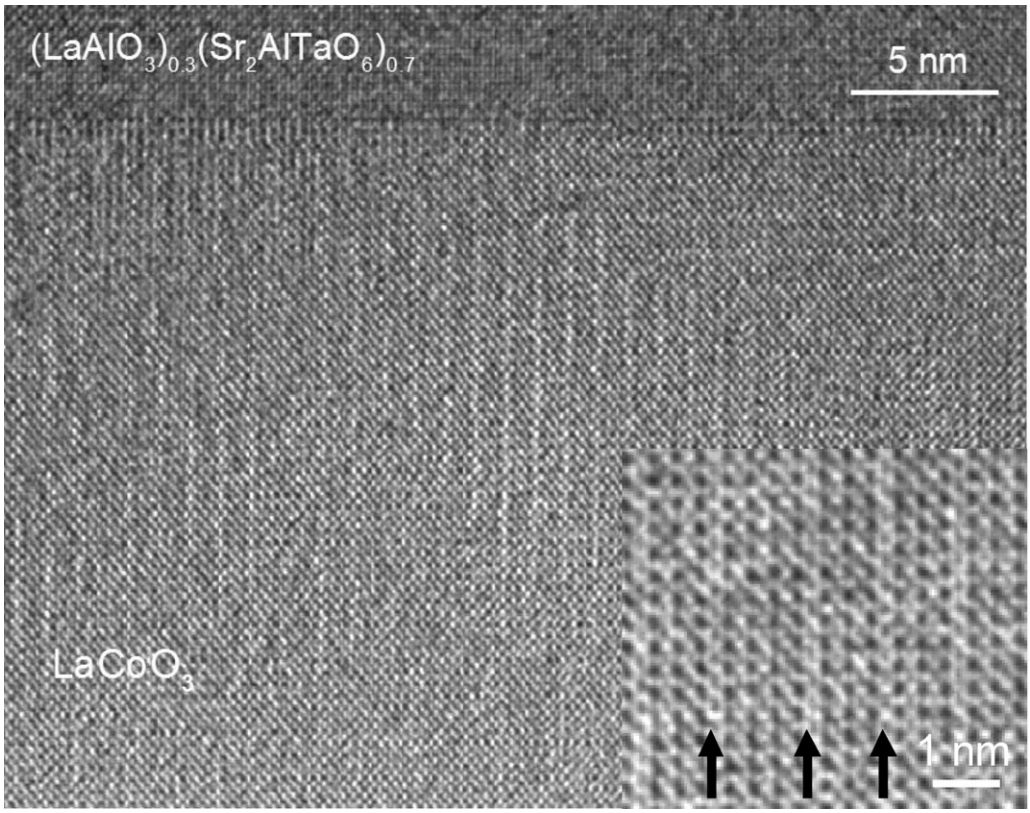

Fig. 6. HRTEM image of $LaAlO_3$ on LSAT; the inset shows an order structure at a higher magnification.

The left-hand side shows an elemental map of La recorded from the same sample with an uncorrected Tecnai F20 using the same experimental parameters (exposure time: 60 s, ~150 electrons/pixel at an energy loss of 860 eV). Figure 8 shows line scans derived from both elemental maps with a line width of ~1 nm. The apparent interface width measured from the uncorrected La map is >2 nm while the C_c-corrected measurement gives an interface width of ~4 Å which is equivalent to the distance of La atoms in $LaCoO_3$. As stated above, the resolution in the C_c-corrected elemental

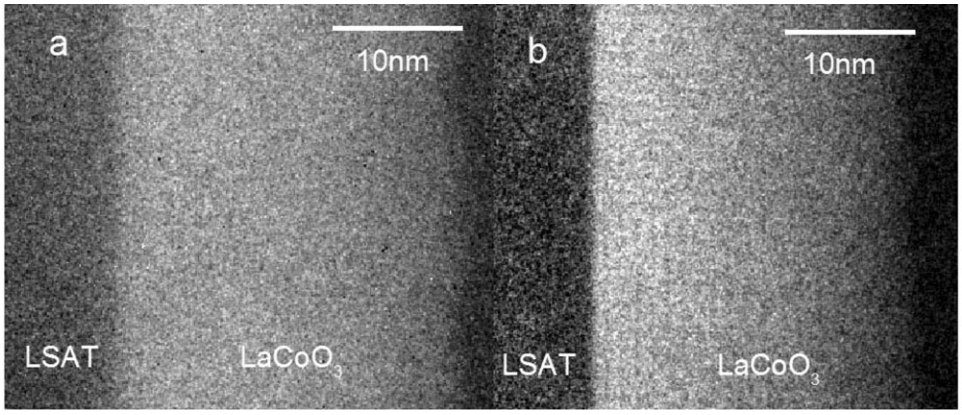

Fig. 7. Elemental maps of La: (a) uncorrected, (b) C_c corrected.

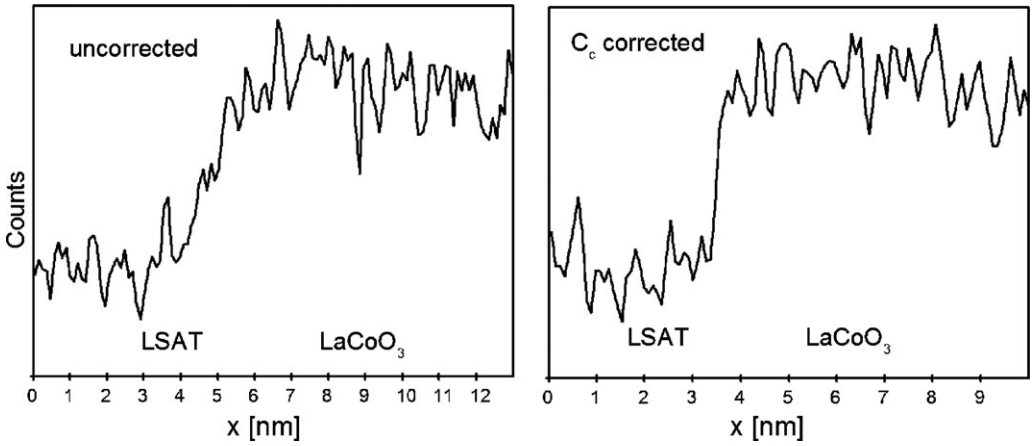

Fig. 8. Line-scans derived from elemental maps of La across the interface LSAT/$LaCoO_3$.

map is limited by the noise and sample drift and we expect further improvement in resolution by using higher beam currents and by minimizing the sample drift.

The resolution improvement in energy-filtered images can be seen without core–shell transitions in the low-loss region too. The coherence of energy-loss electrons from the plasmon peak or from a low-loss EELS transition can enhance resolution despite using a much larger energy selection aperture. Therefore, we placed the energy selection aperture between the plasmon peak and the La–N transition (99 eV) to separate the effect of C_c correction from other influences. The aperture covered the energy range between 45 and 95 eV. Without aberration correction, the contrast from the 4 Å lattice planes is barely visible (Fig. 9a) while with a C_c-corrected instrument ($C_c = 5$ μm, $C_s = 9$ μm, $C_5 = -3$ mm), a high-contrast HRTEM image can be recorded showing details in the perovskite unit cell. The insets in the upper-right corner of the images show Fourier transformations demonstrating the gain in resolution and contrast transfer of C_c correction. The influence of C_s correction on image quality is negligible according to the damping envelopes plotted in Fig. 5. The resolution of the energy-filtered image in Fig. 9b is at least 3.9 Å because the fringes of the (100) and (010) lattice planes are visible in the image as well as in the Fourier transformation. The (110) lattice planes with 2.7 Å are visible in the image and Fourier components can be recognized up to (220). However, it cannot be ruled out that these periodicities are simply an artifact of image formation.

Image formation can be regarded as complex because inelastic as well as elastic scattering contributes to the observed contrast. The delocalization of electrons with an energy loss of 95 eV or less is >1 nm even for a C_c-corrected instrument. Additional elastic scattering of energy-loss electrons can explain the resolution achieved under the assumption that the coherence of these electrons is sufficient for phase contrast imaging. The combination of elastic and inelastic scattering and non-linear image formation requires further investigation to explain the image formation seen in Fig. 9. This imaging mode could be very helpful for improving the resolution attainable for thicker samples where the low-loss region has a higher intensity than the zero-loss beam, which is the case for many biological samples.

Concluding remarks

The potential of C_c correction for HRTEM and EFTEM has been described. According to contrast-transfer calculations, C_c correction is especially effective at lower acceleration

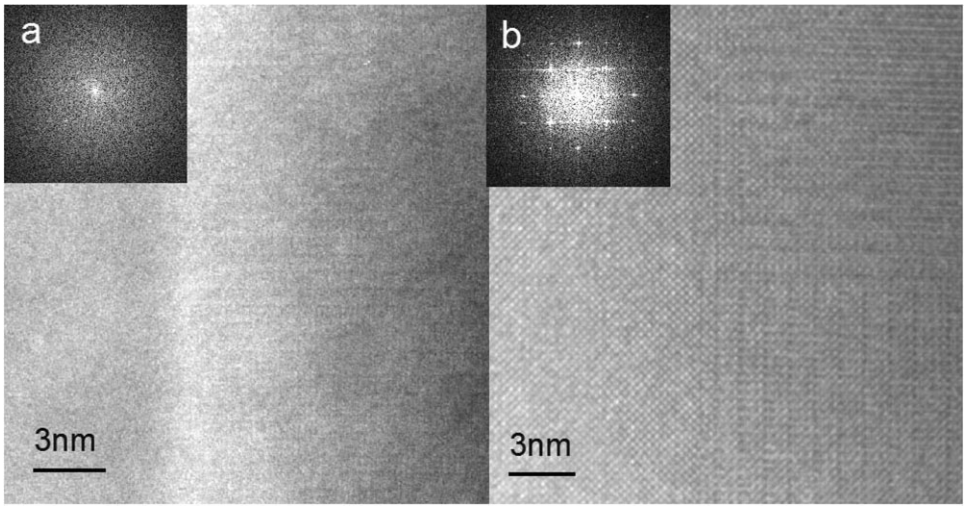

Fig. 9. High-resolution EFTEM in the low energy loss range: (a) uncorrected (b) C_c corrected.

voltages as demonstrated with the first prototype of a C_c corrector. The information limit of an uncorrected or a C_s-corrected instrument without a monochromator can be calculated (and measured) to 1.8 Å. The C_c corrector improves the information limit to 1.0 Å. This is the first time that an aberration correction system has improved the information limit in the TEM mode. Our first C_c-corrected experiments with a cross-sectional thin-film sample demonstrate a large enhancement of resolution in elemental maps derived from energy-filtered images. Chromatic aberration, and to a lower extent spherical aberration, leads to an apparent width of the LSAT/$LaCoO_3$ interface of more than 1 nm as measured from a La elemental map recorded with an uncorrected microscope. A C_c-corrected experiment demonstrates that the La concentration changes within 0.4 nm at this interface (at a distance that is equivalent to the distance between the La planes in $LaCoO_3$). Further experiments in the low-loss region of the energy-loss spectrum with large energy selection aperture demonstrate the strong improvement in resolution that can be achieved using C_c correction for all experiments where the energy width of the electron beam is large. We conclude from this experiment that further benefits of C_c correction can be expected for investigating thick samples that are used in biological or *in situ* TEM studies.

Funding

The submitted work has been created by UChicago Argonne, LLC, Operator of Argonne National Laboratory ('Argonne'). Argonne, a U.S. Department of Energy Office of Science laboratory, is operated under contract no. DE-AC02-06CH11357 as part of the TEAM project, a multilaboratory collaborative effort.

Acknowledgements

The authors thank Levin Dieterle and Dagmar Gerthsen from the University of Karlsruhe for preparation of the $LaCoO_3$ sample.

References

1 Feynman R P (1960) There's plenty of room at the bottom. *Eng. Sci.* **23**: 22–23.

2 BESAC. Review of the Electron Beam Microcharacterization Centers, February 2000. http://www.er.doe.gov/bes/BESAC/e-beam%20report.pdf.

3 Aberration Correction in Electron Microscopy: Materials Research in an Aberration-Free Environment. First TEAM Workshop, Argonne National Laboratory, July 2000. http://ncem.lbl.gov/team/TEAM%20Report%202000.pdf.

4 Materials Research in an Aberration-Free Environment. Second TEAM Workshop, Lawrence Berkeley National Laboratory, July 2002. http://ncem.lbl.gov/team/TEAM%20Report%202002.pdf.

5 Haider M, Rose H, Uhlemann H, Schwan E, Kabius B, and Urban K (1998) Electron microscopy image enhanced. *Nature* **392**: 768–769.

6 Kabius B and Rose H (2008) Novel aberration corrections concepts. *Adv. Imaging Electr. Phys.* **53**: 261–281.

7 Haider M, Muller H, Uhlemann S, Zach J, Loebau U, and Hoeschen R (2008) Prerequisites for a C_c/C_s-corrected ultrahigh-resolution TEM. *Ultramicroscopy* **108**: 167–178.

8 Kisielowski C, Hetherington C J D, Wang Y C, Kilaas R, O'Keefe M A, and Thust A (2001) Imaging columns of the light elements carbon, nitrogen and oxygen with sub Angstrom resolution. *Ultramicroscopy* **89**: 243–263.

9 Linck M, Lichte H, and Lehmann M (2006) Off-axis electron holography: materials analysis at atomic resolution. *Int. J. Mater. Res.* **97**: 890–898.

10 Nellist P D, Chisholm M F, Dellby N, Chisholm M F, Dellby O, Krivanek O L, Murfitt M F, Szilagyi Z S, Lupini A R, Borisevich A, Sides W H Jr., and Pennycook S J (2004) Direct sub-angstrom imaging of a crystal lattice. *Science* **305**: 1741–1741.

11 Reimer L (1984) *Transmission Electron Microscopy*, pp 22 and 220 (Springer, Berlin).

12 Scherzer O (1949) The theoretical resolution limit of the electron microscope. *J. Appl. Phys.* **20**: 20–29.

13 Thust A, Coene W M J, deBeeck M O, and VanDyck D (1996) Focal-series reconstruction in HRTEM: simulation studies on non-periodic objects. *Ultramicroscopy* **64**: 211–230.

14 Ross F M (2006) A unique tool for imaging crystal growth. *Mater. Today* **9**: 54–55.

15 Searson P C, Ross F M, Radisic A, and Vereecken P M (2006) The morphology and nucleation kinetics of copper islands during electrodeposition. *Surf. Sci.* **600**: 1817–1826.

16 Reimer L (1984) *Transmission Electron Microscopy*, p 220 (Springer, Berlin).

17 Uhlemann S (1995) Aufbau und Leistungsgrenzen korrigierter analytischer Transmissions-Elektronenmikroskope. Ph.D. thesis (University of Darmstadt, Germany).

18 Kisielowski C, Freitag B, Bischoff M, van Lin H, Lazar S, Knippels G, Tiemeijer P, van der Stam M, von Harrach S, Stekelenburg M, Haider M, Uhlemann S, Müller H, Hartel P, Kabius B, Miller D, Petrov I, Olson E A, Donchev T, Kenik EA, Lupini A R, Bentley J, Pennycook S J, Anderson I M, Minor A M, Schmid A K, Duden T, Radmilovic V, Ramasse Q M, Watanabe M, Erni R, Stach E A, Denes P, and Dahmen U (2008) Detection of single atoms and buried defects in three dimensions by aberration-corrected electron microscope with 0.5-angstrom information limit. *Microsc. Microanal.* **14**: 454–462.

19 Uhlemann S, and Haider M (1998) Residual wave aberrations in the first spherical aberration corrected transmission electron microscope. *Ultramicroscopy* **72**: 109–119.

20 Kohl H, and Rose H (1985) Theory of image-formation by inellastically scattered electrons in the electron-microscope. *Adv. Imaging Electron Phys.* **65**: 173–227.

21 Krivanek O L, Kundmann M K, and Kimoto K (1995) Spatial resolution in EFTEM elemental maps. *J. Microsc.* **180**: 277–287.

22 Hansteen O H, Fjellvåg H, and Hauback B C (1998) Crystal structure, thermal and magnetic properties of $La_3Co_3O_8$. Phase relations for $LaCoO_{3-\delta}$ ($0.00 < \delta < 0.50$) at 673 K. *J. Mater. Chem.* **8**: 2081–2088.